

Presurgical MR Imaging in Epilepsy

H. Urbach · H. Mast · K. Egger · I. Mader

Received: 28 January 2015 / Accepted: 17 March 2015 / Published online: 8 April 2015
© Springer-Verlag Berlin Heidelberg 2015

Abstract Primary goal of magnetic resonance imaging in epilepsy patients is to detect epileptogenic lesions with small lesions best detectable on a 3D FLAIR SPACE sequence with 1 mm³ voxels. Morphometric analysis of 3D T1-weighted data sets helps to find subtle lesions and may reveal the true extent of a lesion. In further presurgical work-up, language lateralization and spatial relationship of epileptogenic lesions to eloquent cortex and white matter tracts must be evaluated. With clear left lateralization language, fMRI is sufficient; in atypical lateralizations, Wada test and electrical stimulation mapping may be added. Primary motor cortex and corticospinal tract on one and visual cortex and optic radiation on the other side are displayed with fMRI and diffusion tensor tractography. For the corticospinal tract a „global“ tracking algorithm, for the optic radiation including Meyer' loop, which may be damaged in anterior temporal lobe resections, a probabilistic algorithm is best suited.

Keywords Epilepsy · Focal cortical dysplasia · Morphometric analysis · Diffusion tensor tractography

Primary goal of magnetic resonance imaging (MRI) in epilepsy patients is to detect an epileptogenic lesion defined as radiographic lesion that causes seizures [1]. Although the radiologist cannot be sure whether a lesion causes seizures,

there are many lesions typically associated with epileptogenic seizures, that at least the term typically epileptogenic lesion is appropriate.

The effort to search for an epileptogenic lesion depends on the clinical presentation and on the electroencephalography (EEG) findings:

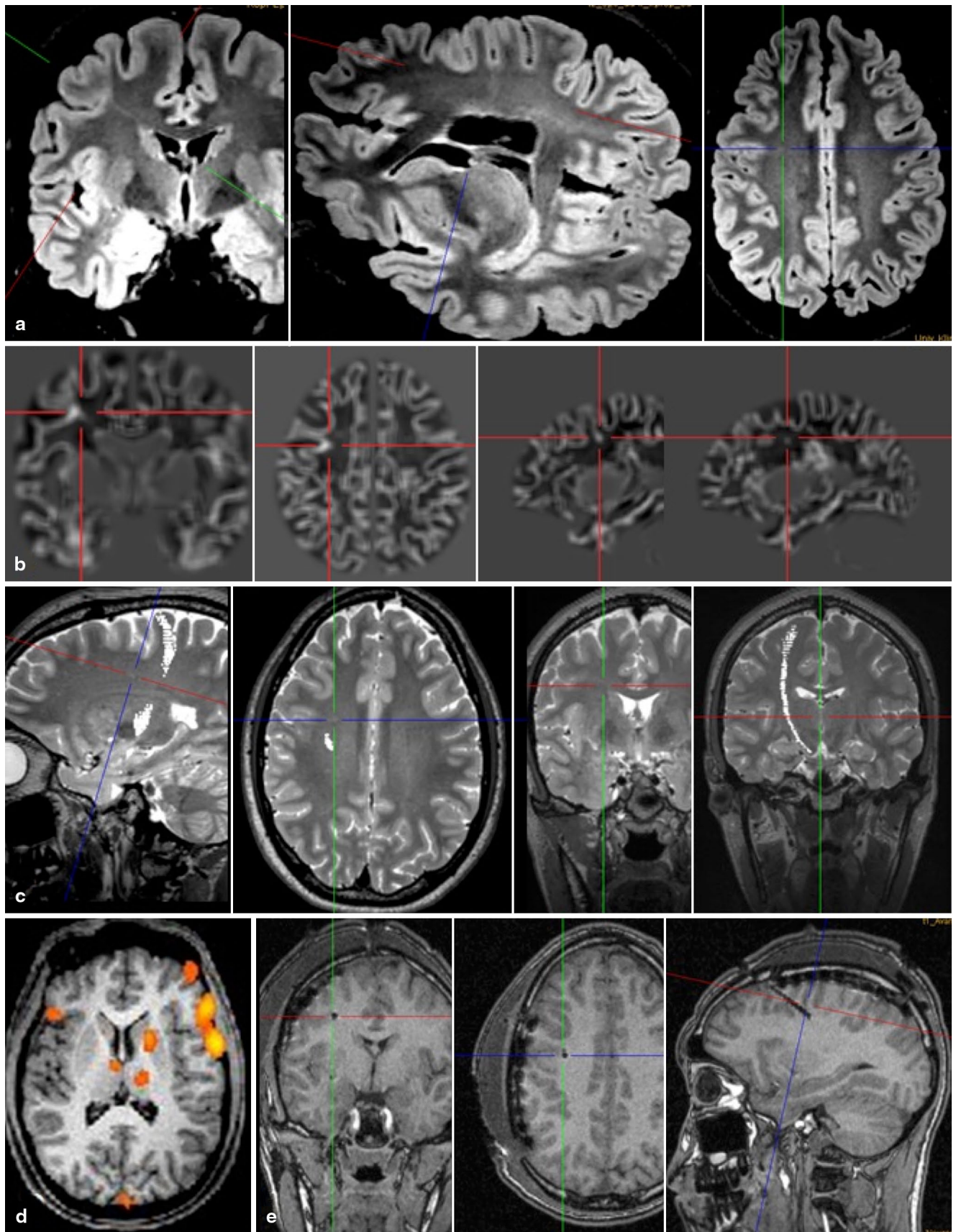
When a patient presents with an acute symptomatic seizure, that is a seizure in the context of an acute disease (trauma, infection, stroke), a standard computed tomography or MRI is sufficient to rule out a disease urgently to treat (ICH, sinus thrombosis, etc.).

When a patient presents with an unprovoked seizure or with an epilepsy syndrome (definition: two unprovoked seizures occurring >24 h apart [2] or one seizure, if paraclinical findings (EEG: e.g., 3/s spike-waves discharges, MRI: e.g., hippocampal sclerosis) point to an increased epileptogenicity) or when a child between 6 months and 5 years of age presents with complex febrile seizures, 1.5- or better 3-T MRI should be performed. The highest effort is targeted to patients with drug-resistant epileptic seizures defined as seizures that persist despite adequate medication with two, tolerated anti-epileptic drugs.

EEG is important, as approximately 40% are primarily generalized or genetic (formerly idiopathic) epilepsy syndromes, in which by definition no underlying structural lesion is present. Typical genetic epilepsy syndromes in childhood include rolandic epilepsy, childhood absence epilepsy, juvenile absence epilepsy, and juvenile myoclonic epilepsy. A typical genetic epilepsy syndrome in adults is wake-up grand mal epilepsy with tonic-clonic seizures typically occurring within the first 2 h after waking-up.

In approximately 60% of cases, epilepsy syndromes are focal, that is epileptic seizures originate within networks limited to one hemisphere: if an epileptogenic lesion is detected, they are classified as structural–metabolic (for-

H. Urbach, MD (✉) · H. Mast · K. Egger, MD · I. Mader, MD, PhD
Department of Neuroradiology,
University Medical Center Freiburg,
Breisacher Str. 64,
79106 Freiburg, Deutschland
e-mail: horst.urbach@uniklinik-freiburg.de



merly symptomatic) epilepsies. If a lesion has not been found (yet), they are classified as cryptogenic epilepsies. The most common focal epilepsy syndrome is temporal lobe epilepsy, and the most common underlying epileptogenic lesion is hippocampal sclerosis. Hippocampal sclerosis was by far the most common finding, when patients were studied with MRI since the late 1980s. Detection rate depended on the exact angulation perpendicular to the hippocampal long axis, and soon the terms “Epilepsy MRI” and “temporal angulation” were used synonymously. Nowadays, hippocampal sclerosis is detected with appropriate 3-T MRI protocols in nearly all cases, and additional automated FLAIR analysis in patients undergoing selective amygdalohippocamectomy indicate that mild hippocampal sclerosis are either difficult to classify neuropathologically or do not exist [3–5]. Interestingly, the incidence of hippocampal sclerosis in large epilepsy surgery centers has significantly decreased during the past decade; the incidence of long-term epilepsy-associated tumors is also declining, while the incidence of focal cortical dysplasias (FCDs) increases [6]. FCDs are often small, they do not change during life and in many instances have been overlooked for years (Fig. 1). To detect them the radiologist needs clinical information, especially about the semiology of the seizures pointing to the region in which the seizure likely originate. MRI examination must be a reasonable compromise between spatial resolution and signal/noise or contrast/noise ratio acknowledging that epilepsy patients are often uncooperative and will not tolerate “long” sequences. In a rank analysis of MRI sequences suited for the detection of epileptogenic lesions, cumulative percentage of lesion entities detected after the first to fifth sequence were 84.8% for FLAIR, 91.6% for coronal T2-weighted (w) fast spin-echo or STIR, 97.4% for T2*, 99.4% for T1-w or inversion recovery, and 100% for contrast-enhanced T1-w sequences. After FLAIR, T2/STIR, T2*, and T1-w sequences, 99.4% of all lesions and all lesion types were detected except for subtle pial angiomatosis [7]. Therefore, a 3-T MRI protocol including the following sequences (Table 1) has been proposed, this protocol is also suggested to be used in an outpatient clinic [7]. Of note, due to ongoing myelination, FLAIR sequences are of little value in the first 3 years of life: during this period, T1-w and T2-w sequences focusing on a high signal/noise ratio are preferred.

When an epileptogenic lesion has not been found, but semiology of the seizures and EEG findings clearly point to a focal seizure onset, morphometric analysis of the

3D-T1-w (or 3D-T2, 3D-FLAIR) data sets can be helpful (Fig. 1). Briefly, after spatial normalization, segmentation, smoothing, and comparison with a large reference population examined by the same imaging protocol, three parameter maps displaying the cortical thickness and the extension of the cortex into the white matter and the gray–white junction are highlighted [8]. Of note, if a small FCD is highlighted by morphometric analysis, the MR images must be carefully re-inspected: the lesion must also be visible on the MRI data sets, otherwise it is a false-positive lesion. This means morphometric analysis is an elegant tool to find a “nearly invisible” and thus overlooked FCD, it may also show the true extension of a lesion [9, 10]

When an epileptogenic lesion has been identified, its spatial relationship to eloquent cortex and white matter tracts must be clarified. In many epileptogenic lesion, not only the lesion itself but also perilesional tissue constituting the epileptogenic zone (definition: area of cortex indispensable for the generation of seizures [1]) must be resected to achieve seizure freedom. The following procedures are incorporated in a standardized presurgical work-up:

1. fMRI for language lateralization (Fig. 1)

For language fMRI, we apply a block-design experiment (TR 2500 ms, TE 30 ms, 41 axial slices, matrix size 64×64 pixels, voxel size $3 \times 3 \times 3$ mm³, 136 volumes, 8 volumes activation, 8 volumes rest, acquisition time 5:40 min) with at least two different tasks: a language production task consisting of verb generation as task versus visually presented nouns as rest condition; a language comprehension test of synonyms recognition versus parallelized color comparison. Results are computed with thresholds > 0.4 and 0.5 and final assessment also considers the handedness as addressed with the Edinburgh handedness score [11].

fMRI shows left lateralization in $> 90\%$ of healthy individuals, but only approximately 78% of epilepsy patients. Bilateral (approximately 16%) or right lateralization (approximately 6%) is more common in epilepsy patients and associated with an earlier age of brain injury and with weaker right-hand dominance [12]. fMRI can reliably detect strongly left-lateralized language. In a meta-analysis comparing fMRI with the Wada test as gold standard for preoperative assessment of lateralization of language and memory function, fMRI and Wada test agreed in 94% for typical language lateralization and in 51% for atypical language lateralization [13]. This means, if fMRI clearly shows left lateralization of language, the test is sufficient. If fMRI does not show left-lateralized language clearly, confirma-

Fig. 1 Presurgical work-up in an 18-year-old patient with drug-resistant epilepsy likely originating in the right frontal lobe. An isotropic 3D FLAIR SPACE sequence with 1 mm³ voxels shows a small transmantle sign in the depth of the middle frontal gyrus (a: *crosshair*). Morphometric analysis of the 3D MPRAGE sequence confirms the subtle signal abnormality (b). Diffusion tensor tractography shows the corticospinal tract 8 mm dorsal to the lesion (c). A word generation task shows left-sided language representation with little co-activation in the right inferior frontal gyrus (d). 1.5-T magnetic resonance imaging following implantation of subdural end depth electrodes shows the depth electrode with its tip at the lesion (e)

Table 1 Magnetic resonance imaging protocol for patients with focal epilepsy syndromes

Number	Acquisition time (min)	Sequence	Orientation/slice thickness	Diagnostic yield
1	~7	3D T1-weighted (w) FFE or MPRAGE	Sagittal (sag)/1 × 1 × 1 mm ³	Multiplanar reformatting Voxel-based morphometry
2	~4–5	2D T2-w TSE	Axial (ax)/3–5 mm	Exact angulation
3	~7–10	3D FLAIR VISTA or SPACE	sag/1 × 1 × 1 mm ³	Focal cortical dysplasias HS
	Altern. 5	2D FLAIR-TSE and	ax/2–3 mm	
	Altern. 5	2D FLAIR-TSE	Coronal (cor)/2–3 mm	
4		2D T2-w TSE	cor/2–3 mm	HS
5	~3	SWI or 2D-FFE	ax/1.5–5 mm	Cavernoma, hemosiderin
6	~5	3D T1-w FFE or MPRAGE+contrast	sag/1 × 1 × 1 mm ³	Tumor (long-term epilepsy-associated tumors)

HS hippocampal sclerosis

tion with other techniques such as the Wada test or electrical-stimulation mapping is needed [13].

2. fMRI for localization of primary motor or visual cortex and diffusion tensor tractography for visualization of the pyramidal tract (Fig. 1) or optic radiation

The pyramidal tract or optic radiation are calculated from a single-shot SE-EPI DWI sequence (TR, 10 s; TE, 94 ms; voxel size, 2 mm³; 61 diffusion-encoding directions; effective b-value, 1000 s/mm²).

For the pyramidal tract, two seed points in the precentral gyrus and ipsilateral crus cerebri are selected. The precentral gyrus is identified via fMRI (TR, 2.5 s; TE, 30 ms, 3 × 3 × 3 mm³, active fist clenching and tongue movement versus rest, 1 Hz, 8 measurements) or automated parcellation with the FreeSurfer (<http://surfer.nmr.mgh.harvard.edu/>) algorithm [14]. Brain stem seed points are derived from a voxel-based atlas [15].

The deterministic fiber assignment by continuous tractography (FACT) algorithm [16] (stopping criteria: fractional anisotropy >0.1, curvature between 2 consecutive steps ≥90°) is normally sufficient to display the pyramidal tract; however, a global tracking algorithm reconstructs a wider fan of descending motor fibers, which are most likely missed by the FACT algorithm due to crossing fibers of the superior longitudinal fascicle and corpus callosum [17, 18].

For the optic radiation, two seed points in the pericalcarine cortex and lateral geniculate ganglion are selected. A four-quadrant visual field stimulation paradigm identifies the pericalcarine cortex, and a probabilistic tracking algorithm is best suited to display the inferior or ventral bundle of the optic radiation. This bundle known as Meyer's loop makes a wide anterior and lateral loop around the temporal horn of the lateral ventricle and is particularly vulnerable to damage during anterior temporal lobe resections with between 48 and 100% of patients experiencing a postoperative contralateral superior quadrantanopia that precludes driving in 4–50% of patients even if seizure free [19]. In a series of 10 patients, the mean distance between the tempo-

ral pole and the tip of the Meyer's loop was 34 mm with a range from 23.1–40 mm [18]. Here, we use an extension to the probabilistic index of connectivity method, which calculates not only the probability that a voxel is connected to the selected ROI by performing random walk iterations and counting the visits but also considers the directional information of the curves passing through the voxel [20, 21]. The probability information of voxels receiving visits from opposing directions creates probabilistic maps of connectivity. Parameters used are 10⁵ random walk iterations from every seed region voxel and applying an exponent of 4 to the eigenvalues, whereas the stopping criterion was FA >0.1.

Ideally, activated voxel and calculated white matter tracts are coregistered to the 3D T1-w data set and stored into a neuronavigation system. To date, this is only allowed for the FACT algorithm (Fig. 1), while probabilistic and global algorithm have no CE or Food and Drug Administration approval yet.

Other tools are complementarily used to depict the interictal zone (¹⁸FDG-PET, EEG-fMRI) or are a topic of research (resting state fMRI, MR encephalography). If these noninvasive tools together give no hint on the epileptogenic zone, intracranial EEG recordings and electrical stimulation mapping via subdural or depth electrodes are considered [22]. Here, the exact visualization of the electrode contacts are again task of the neuroradiologist (Fig. 1) [23].

Conflict of interest The authors declare that there are no actual or potential conflicts of interest in relation to this article.

References

- Rosenow F, Lüders H. Presurgical evaluation of epilepsy. *Brain*. 2001;124:683–1700.
- Fisher RS, Acevedo C, Arzimanoglou A, Bogacz A, Cross JH, Elger CE, Engel J, Jr., Forsgren L, French JA, Glynn M, Hesdorffer DC, Lee BI, Mathern GW, Moshé SL, Perucca E, Scheffer

- IE, Tomson T, Watanabe M, Wiebe S. A practical clinical definition of epilepsy. *Epilepsia*. 2014;55:475–82.
3. Blümcke I, Thom M, Aronica E, Armstrong DD, Bartolomei F, Bernasconi A, Bernasconi N, Bien CG, Cendes F, Coras R, Cross JH, Jacques TS, Kahane P, Mathern GW, Miyata H, Moshé SL, Oz B, Özkara Ç, Perucca E, Sisodiya S, Wiebe S, Spreafico R. International consensus classification of hippocampal sclerosis in temporal lobe epilepsy: a task force report from the ILAE commission on diagnostic methods. *Epilepsia*. 2013;54:1315–29.
 4. Bien CG, Szinai M, Wagner J, Clusmann H, Becker AJ, Urbach H. Characteristics and surgical outcome of patients with refractory MRI-negative epilepsies. *Arch Neurol*. 2009;66:1491–9.
 5. Urbach H, Huppertz HJ, Schwarzwald R, Becker AJ, Wagner J, Delsous Bahri M, Tschampa HJ. Is the type and extent of hippocampal sclerosis measurable on high-resolution MRI? *Neuroradiology*. 2014;56:731–5.
 6. Bien CG, Raabe AL, Schramm J, Becker A, Urbach H, Elger CE. Trends in presurgical evaluation and surgical treatment of epilepsy at one centre from 1988–2009. *J Neurol Neurosurg Psychiatry*. 2013;84:54–61.
 7. Wellmer J, Quesada CM, Rothe L, Elger CE, Bien CG, Urbach H. Proposal for a magnetic resonance imaging protocol for the detection of epileptogenic lesions at early outpatient stages. *Epilepsia*. 2013;44:1977–87.
 8. Huppertz HJ. Morphometric MRI analysis. In: Urbach H, Editor. *MRI in epilepsy*. New York: Springer Heidelberg; 2013. pp. 73–84.
 9. Wagner J, Weber B, Urbach H, Elger CE, Huppertz HJ. Morphometric MRI analysis improves detection of focal cortical dysplasia type II. *Brain*. 2011;134(Pt 10):2844–54.
 10. Huppertz HJ, Wellmer J, Staack AM, Altenmüller DM, Urbach H, Kröll J. Voxel-based 3D MRI analysis helps to detect subtle forms of subcortical band heterotopia. *Epilepsia*. 2008;49(5):772–85.
 11. Oldfield RC. The assessment and analysis of handedness. *Neuropsychologia*. 1971;9:97–113.
 12. Springer JA, Binder JR, Hammeke TA, Swanson SJ, Frost JA, Bellgowan PS, Brewer CC, Perry HM, Morris GL, Mueller WM. Language dominance in neurologically normal and epilepsy subjects. *Brain*. 1999;122:2033–45.
 13. Bauer P, Reitsma JB, Houweling BM, Ferrier CH, Ramsey NF. Can fMRI safely replace the Wada test for preoperative assessment of language lateralisation? A meta-analysis and systematic review. *J Neurol Neurosurg Psychiatry*. 2014;85(5):581–8.
 14. Destrieux C, Fischl B, Dale A, Halgren E. Automatic parcellation of human cortical gyri and sulci using standard anatomical nomenclature. *Neuroimage*. 2010;53:1–15.
 15. Maldjian JA, Laurienti PJ, Kraft RA, Burdette JH. An automated method for neuroanatomic and cytoarchitectonic atlas-based interrogation of fMRI data sets. *Neuroimage*. 2003;19:1233–9.
 16. Mori S, Crain BJ, Chacko VP, van Zijl PC. Three-dimensional tracking of axonal projections in the brain by magnetic resonance imaging. *Ann Neurol*. 1999;45:265–9.
 17. Reisert M, Mader I, Anastasopoulos C, Weigel M, Schnell S, Kiselev V. Global fiber reconstruction becomes practical. *Neuroimage*. 2011;54:955–62.
 18. Anastasopoulos C, Reisert M, Kiselev VG, Nguyen-Thanh T, Schulze-Bonhage A, Zentner J, Mader I. Local and global fiber tractography in patients with epilepsy. *AJNR Am J Neuroradiol*. 2014;35:291–6.
 19. Winston GP, Daga P, Stretton J, Modat M, Symms MR, McEvoy AW, Ourselin S, Duncan JS. Optic radiation tractography and vision in anterior temporal lobe resection. *Ann Neurol*. 2012;71:334.
 20. Parker GJ, Haroon HA, Wheeler-Kingshott CA. A framework for a streamline-based probabilistic index of connectivity (PICO) using a structural interpretation of MRI diffusion measurements. *J Magn Reson Imaging*. 2003;18:242–54.
 21. Kreher BW, Schnell S, Mader I, Il'yasov KA, Hennig J, Kiselev VG, Saur D. Connecting and merging fibres: pathway extraction by combining probability maps. *Neuroimage*. 2008;43:81–9.
 22. Ryvlin P, Cross JHM, Rheims S. Epilepsy surgery in children and adults. *Lancet Neurol*. 2014;13:1114.
 23. Kovalev D, Spreer J, Honegger J, Zentner J, Schulze-Bonhage A, Huppertz HJ. Rapid and fully automated visualization of subdural electrodes in the presurgical evaluation of epilepsy patients. *AJNR Am J Neuroradiol*. 2005;26:1078–83.